

Preparation of carbon-coated metal particles and their electrochemical performance

Zixuan Fang¹, Zhiwen Xu¹, Lun Xiong^{1*}, Huan Wang¹, Hongyang Zhao^{1*},
Linyong Huang^{1,2}, Zhibin Ma^{1,2}

¹ School of Optical Information and Energy Engineering, Key Laboratory of Plasma Chemical and Advanced Materials of Hubei Province, Wuhan Institute of Technology, 206, Guanggu 1st Road, Wuhan 430205, China.

² Huanggang Normal University, Huanggang 436100, China.

Corresponding Author: Lun Xiong, Hongyang Zhao

ABSTRACT: In this paper, carbon-coated with different transition metal particles were prepared by hydrothermal carbonization and acid etching processes using nickel, copper, cobalt, and iron acetates and glucose as raw materials, respectively. The formation mechanism, structure, and electrochemical properties were studied. XRD, SEM and EDS results showed that carbon-coated metal particles and their perfect core-shell structure in metal particles. The double-layer capacitance properties were investigated by electrochemical tests as well. The results showed that the Ni/C metal particles exhibited more excellent electrochemical capacitance, higher rate performance and low electrolyte ionic resistance characteristics. The superior performance can be attributed to the large specific surface area and the enhanced electrical conductivity of the material after coating the nickel metal particles. These findings are significant for understanding the mutual modulation between the microstructure and electrochemical properties of high-capacity particles materials.

Keywords: carbon coating; transition metal; particle; electrochemical performance

Date Of Submission: 09-05-2019

Date Of Acceptance: 24-05-2019

I. INTRODUCTION

Carbon-coated metal particles (CCMPs) are a composite material composed of carbon and metal, which is closely composed of several layers of graphite tightly coated with metal particles. The particles can be tightly fixed in a small space, which has a good protective effect and solves the environmental impact on metal particles. Owing to its special carbon-coated core-shell structure and unique particle size, such as the large proportion of interface units, small size effect and interface effect, the CCMPs have excellent electrochemical performance (high conductivity, high dielectric).

With the rapid development of core-shell nanomaterials [1, 2], modern industry has higher requirements for sensitivity, reliability, integration and multi-functionality in conducting devices. CCMPs have also been widely concerned and studied in the field of photocatalysis [3-5]. There are many methods to prepare metal nanomaterials for conductive applications, such as arc discharge [6], hydrothermal method [7], chemical vapor deposition [8], laser technology [9], which are highly designed in adjustable parameters. The size structure and size of metal nanomaterials can be controlled by adjusting metal source materials, reaction temperature and calcination time. At present, carbon-coated metal materials are difficult

to maintain high capacitance when the overall size of capacitors is reduced, and there is a problem that nanoparticles affect their specific capacitance [10]. Very recently years, in order to improve the electrochemical performance of power supply, the choice of different carbon precursors and metal ions has been extensively studied [11-15]. Meanwhile, the possibility of heteroepitaxy growth of diamond films was explored worthily by using the similar lattice structure and constants of Ni, Co and other diamonds.

Hence, we prepared CCMPs by hydrothermal synthesis using nickel (Ni), copper (Cu), cobalt (Co), iron (Fe) acetate and glucose, respectively. The results show that the core-shell structure with large specific surface area, size and interface effect can significantly improve the conductivity and dielectric properties. The microstructures of the synthesized particles were observed by scanning electron microscopy (SEM). The crystal structure and composition were studied by X-ray diffraction (XRD). The capacitance and dielectric properties of the materials were also studied, and the formation mechanism was discussed.

II. EXPERIMENTAL DETAILS

2.1 Sample preparation

CCMPs were synthesized by dissolving 1.23 g Ni acetate tetrahydrate (copper, cobalt, ferrous) powder and 0.99 g glucose powder in 70.0 mL distilled water. The mixture was transferred to the reactor and placed in 180 °C constant temperature treatment. After filtration, precipitation and washing, the products were collected and dried in a 70 °C drying furnace. The drying time was controlled according to the amount of samples. Sample "a" is calcined at 700 °C for 3 hours in nitrogen atmosphere at a heating rate of 2 °C/min. At this time, the product is transformed into Ni (Cu, Co, Fe)/C composite material, called sample "b". Finally, sample "b" was added with appropriate amount of concentrated of hydrochloric acid (concentration of 37%) and placed in the reactor again, which is treated at 180 °C for 24 hours. After cooling, centrifugation was carried out and ethanol was used for cleaning. Finally, followed by heat treatment in a 70 °C drying oven, called sample "c", was the preparation of carbon-coated metal particle composites.

2.2 Characterization

X-ray Diffraction (XRD) was measured by Shimadzu XRD-6100. The surface morphology and core-shell structure of the powder samples were observed by Scanning Electron Microscope (SEM) and elemental analysis using an energy spectrometer (Energy Dispersive Spectrometer, EDS) EDS-Model 550i for qualitative and quantitative analysis. The specific surface area and morphology of the sample were determined by Quantachrome QUADRASORB SI type surface area meter, and the specific surface area of the sample was calculated according to the BET theoretical model test formula. The pore size distribution and other performance parameters of the sample were tested according to the BJH model. The electrochemical properties were examined by a CHI760E series electrochemical analyzer or workstation general electrochemical system.

III. RESULTS AND DISCUSSION

3.1 Formation mechanism analysis

The formation mechanism in this experiment is different from the traditional dissolution-precipitation mechanism and cooling crystallization mechanism, as shown in Fig. 1. During the reaction, Ni acetate plays a variety of roles, such as: the inducer stratifies the carbon as a graphitization catalyst and a pore former [16, 17]. First, Ni(OH)₂ was formed by forced hydrolysis of Ni acetate at high temperature. Due to the hydrogen bond, glucose was easily hydrothermal polymerized to form the polysaccharides, which were coated on the surface of Ni(OH)₂ to form a flower-like Ni(OH)₂/polysaccharide microspheres.

Then they were calcined at 700 °C in a tubular furnace and carbonized to constitute a carbon-coated nickel (Ni/C) composite structure. Finally, the residual Ni metal particles formed the flower-like layered mesoporous carbon structure (FMCS) after the precursor Ni(OH)₂/polysaccharide microspheres were moved by hydrochloric acid and treated by carbonization [8].

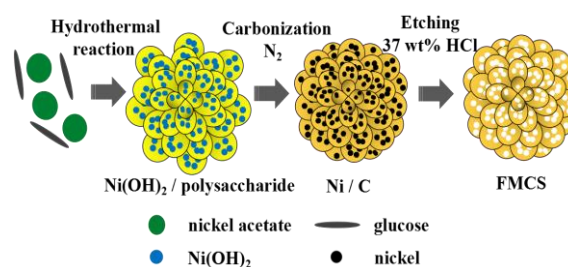


Fig. 1 Formation mechanism of Ni/C particles

3.2 Phase Analysis

Fig. 2 (a-d) is the XRD patterns of carbon-coated Ni (Cu, Co, Fe) metal particles, and the black curve is sample "b", which is a flower-like Ni(OH)₂(Cu(OH)₂, Co(OH)₂, Fe(OH)₂)/polysaccharide microsphere. There are mainly three main characteristic diffraction peaks in the figure, which are Ni (Cu, Co, Fe). (111), (200) and (220) lattice planes whose position and intensity are consistent with the corresponding standard cards (JCPDS No. 04-0850, No. 04-0836, No. 15-0806, No. 85-1410), indicating that the main component of the Ni/C product is Ni, the main component of the carbon-coated copper (Cu/C) product is Cu, the main component of the carbon-coated cobalt product is Co, and the main component of the carbon-coated iron (Fe/C) product is Fe, and both belong to the surface. In the heart-cube crystal system, no other impurity phase was observed. It is clearly reflected that the reaction is complete when the sample "b" is carbonized, and no by-products such as corresponding metal carbides, metal oxides, and ferrite are acquired.

The red curve in the graph (a-c) is the XRD pattern of the experimental sample "c", Ni/C (Cu/C, Co/C, Fe/C) achieved after treatment with HCl solution. It can be clearly seen that the characteristic peaks of Ni (Cu, Co, Fe) disappear, and the corresponding (120) and (111) lattice planes appear in the vicinity of 2θ = 26.4° and 43°, indicating that there are significant carbon diffraction peaks. Since hydrochloric acid is sufficiently washed with Ni (Cu, Co, Fe) to form the solution, eventually leaving the desired nanoparticle carbon coating structure.

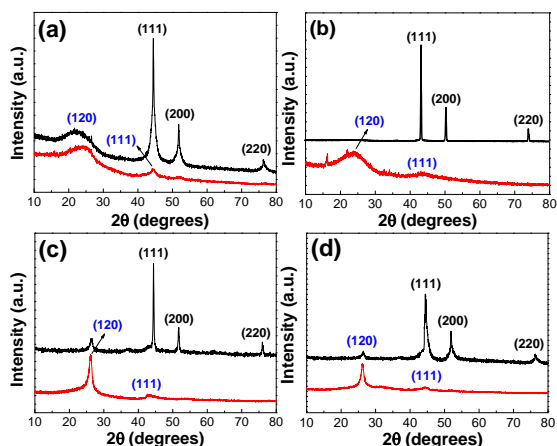


Fig. 2 XRD patterns of carbon-coated (a) Ni, (b) Cu, (c) Co, (d) Fe metal particles (sample “b”, black curve; sample “c”, red curve).

3.3 Morphology and EDS spectrum analysis

Fig. 3 (a-d) is the SEM images of carbon-coated Ni (Cu, Co, Fe) metal particles. It can be seen from the figure that the particles are substantially spherical and the edges are clear, showing a more uniform nucleation morphology. What reflects in Fig. 3 (a) is that the particles are randomly gathered together with the relatively uniform particle size distribution. The particle dispersion is good, and there is a slight agglomeration phenomenon. This spherical agglomeration arrangement is due to the interaction of the nanoparticles with the magnetic force and surface tension between the ultrafine particles [11]. Compared with those uncoated, the surface of the particles is rough but displays a good spherical shape. The particles are coated with a carbon shell layer with the relatively uniform thickness, and the thin layer of the outer shell belongs to an amorphous carbon coating film. It can be clearly seen from the figure (b-c) that the flower-like precursor consists of a very thin carbon film [18] with many well-dispersed particles embedded in the edges. Fig. 3 (d) shows the SEM image of residual Fe metal particles after the precursor is removed by hydrochloric acid and treated by carbonization. Finally, a flower-like layered mesoporous carbon structure (FMCS) is constituted. The above test structure is basically consistent with the diffraction spectrum obtained by the Ni/C metal particle sample in Fig. 2.

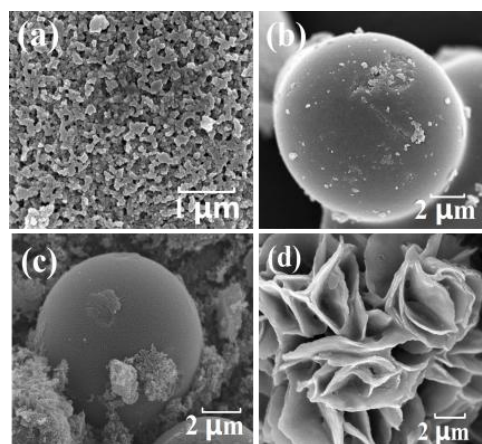
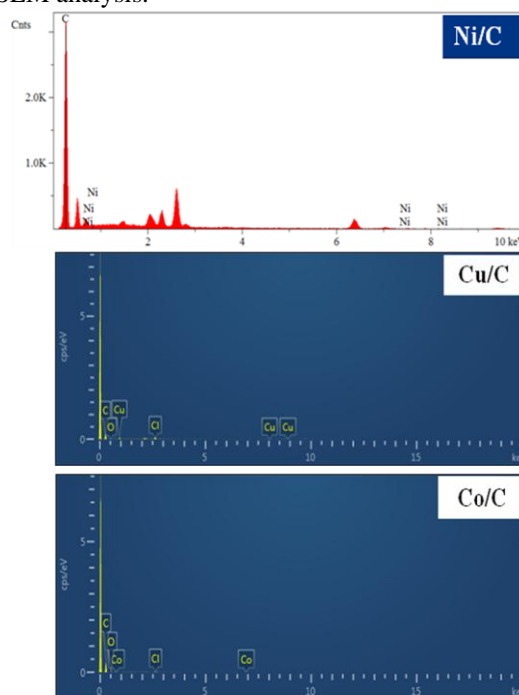


Fig. 3 SEM images of carbon-coated (a) Ni, (b) Cu, (c) Co, (d) Fe metal particles.

Additionally, the above CCMPs were further analyzed by EDS element analysis, selection of elements and the corresponding content of elements in micro-areas. Fig. 4 is the corresponding EDS spectra. The analysis shows that most of the shell structures of coated Ni (Cu, Co, Fe) particles are corresponding Ni (Cu, Co, Fe) elements except element C, and a very small amount of oxygen exists at the same time. The analysis results further show that the core of the sample is the metal element corresponding to the coating carbon shell. There is an obvious core-shell structure, which is consistent with the results of SEM analysis.



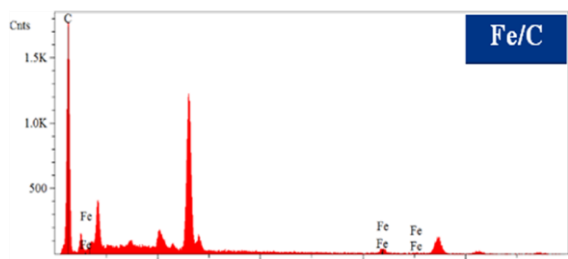


Fig. 4 EDS energy spectrum images corresponding to carbon-coated metal particles (Ni/C, Cu/C, Co/C, Fe/C)

3.4 Specific surface area and pore size distribution

The N_2 adsorption pore size distribution of carbon-coated Ni (Cu, Co, Fe) metal particles obtained by BJH is shown in Fig. 5, and the inner graph is the corresponding N_2 adsorption-desorption isotherm. The narrow pore diameter curve indicates that the pore size distribution is relatively concentrated, mainly for micropores and mesopores. The pore size of the sample is distributed in the range of 30-100 nm. The obvious peak value of Ni/C in the figure near 37 nm (Cu/C at 98 nm, Co/C at 56 nm, Fe/C at 35 nm) indicates that the pore with the corresponding diameter of 37 nm (98 nm, 56 nm, 35 nm) accounts for the largest proportion in the sample. According to BJH theoretical model, the average pore size of carbon-coated Ni (Cu, Co, Fe) particles for BJH adsorption is 6.98 nm (3.87 nm, 1.75 nm, 1.34 nm).

The internal diagram exhibits that the carbon-coated Ni (Co, Fe) isotherms are typical of the Langmuri IV type. The low-pressure zone has less adsorption and no inflection point, and the adsorption-desorption curve is very close and almost coincident, indicating the micropores (<2 nm) of the particles. The ratio is higher, and the adsorption of the initial part of the isotherm mainly occurs in the micropores, which is limited to the film obtained on the crucible. It indicates that the sample has a single pore size distribution and a certain mesoporous (2~50 nm) large pore structure. The specific surface area S_M of the carbon-coated Ni (Cu, Co, Fe) metal particles were 241.08 m^2/g , 43.94 m^2/g , 61.32 m^2/g , and 187.86 m^2/g , which is measured by BET multilayer gas adsorption method. The specific surface area of Ni/C samples was the largest.

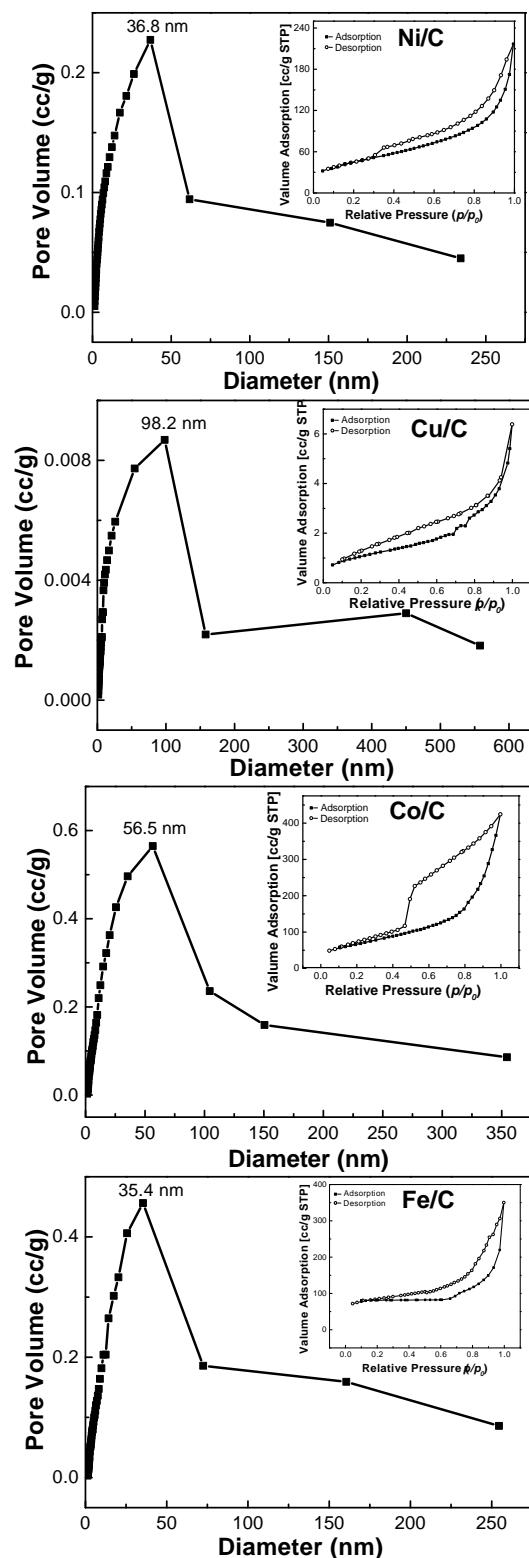


Fig. 5 BJH adsorption pore size distribution of carbon-coated Ni (Cu, Co, Fe) metal particles, the inner picture shows the corresponding adsorption and desorption curve.

3.5 Electrochemical performance

Electrochemical capacitance performance of carbon-coated transition metal particles three-electrode system is used in the CHI760E

electrochemical test system (1 mol/L electrolyte). The Na_2SO_4 solution was subjected to Cyclic Voltammetry (CV), Constant Current Charge Discharge (CD) and Electrochemical Impedance Spectroscopy (EIS) tests. It can be clearly seen in Fig. 6 (a) that the CV curve presents a parallelogram (rectangular shape) shape, showing a typical double-layer capacitance characteristic. It remains a similar parallelogram (rectangular) shape when the scanning rate is increased from 10 mV/s to 200 mV/s, indicating excellent capacitance performance. The fast movement of electrolyte and ion at the interface makes charge propagate well between electrolyte and carbon material. CD curves on the Fig. 6 (b) shows that all the quasi-isosceles triangles are displayed at different current densities. Its outstanding coulomb efficiency and ideal capacitor effect are demonstrated.

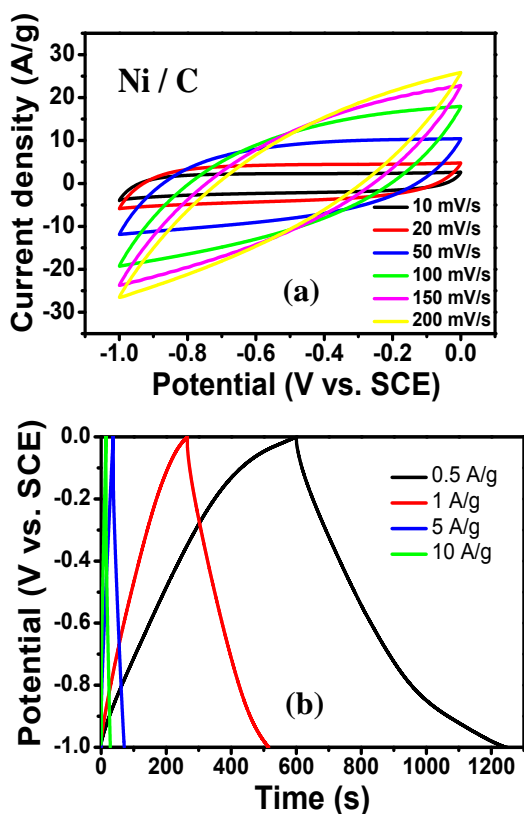
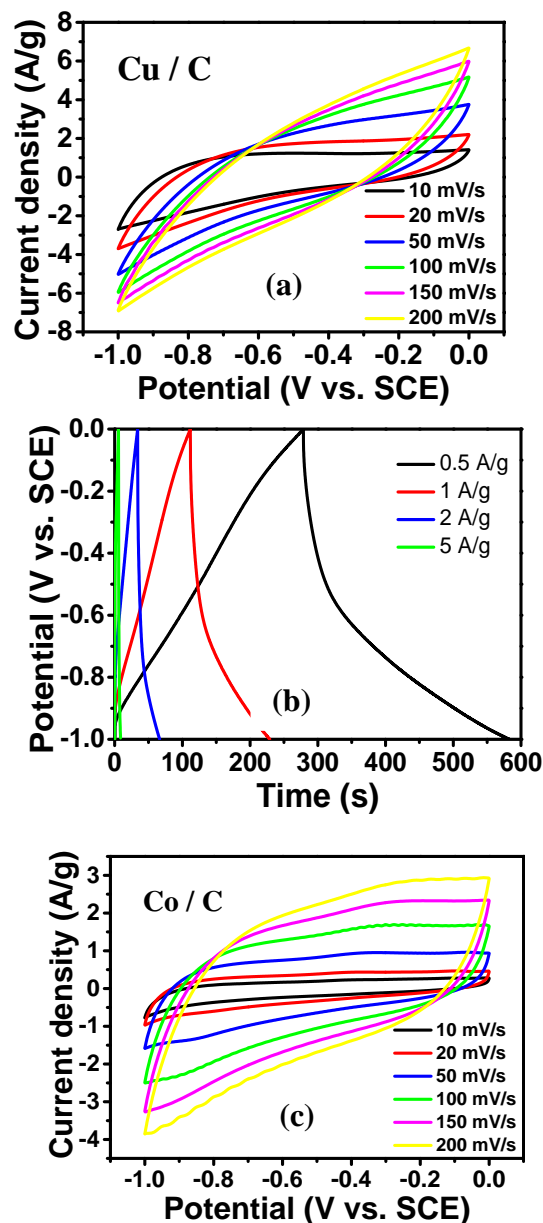


Fig. 6 Ni/C metal particles (a) cyclic voltammograms based on electrodes at different scan rates and (b) charge-discharge curves based on different current densities.

The charge-discharge efficiency of supercapacitor [19] is about 100%, and its charge-discharge curve is isosceles triangle. In this experiment, the capacities of the electrodes vary with the potential of the electrodes, so the final CD curve will be slightly bent. Under constant current charging and discharging conditions, it is obvious that there is a specific linear relationship between

voltage and time, which indicates that the electrode reaction in this process is mainly charge transfer reaction on double capacitors. In order to make the experiment more convincing, the same molar weight of cobalt acetate, copper acetate and ferric acetate reagents were selected to prepare Cu/C, Co/C, Fe/C metal particles under the resembled conditions, and their CV and CD curves were measured. The specific test results are shown in Fig. 7.



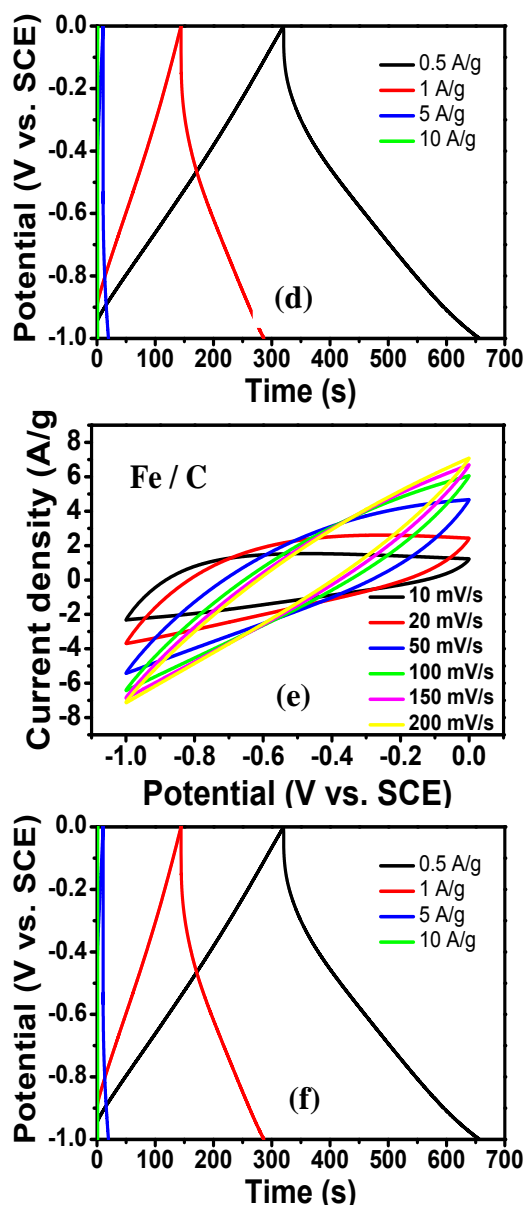


Fig. 7 (a), (b) CV and CD curves of Cu/C particles; (c), (d) CV and CD curves of Co/C particles; (e), (f) CV and CD curves of Fe/C particles.

From the analysis and comparison of Fig. 7, it can be concluded that the cyclic volt-ampere characteristic curves of all carbon-coated metal (Cu, Co, Fe) particles at various scanning rates are the same as Ni/C. This particles exhibit the similar rectangular structure, thus better demonstrating that carbon-coated metal particulate materials have typical double-layer capacitance characteristics [20]. The constant current charge and discharge curves are similar, so it can be inferred that the granular materials have good rate performance. According to the analysis of the charge and discharge data, the specific capacitance of the corresponding sample can be obtained. The calculation formula is as followed:

$$C = I\Delta t / m\Delta U$$

(1)

Wherein I is a charge and discharge current (A), t is a charge or discharge time (s), ΔU is a voltage change amount (V), and m is a single electrode active material mass (g). When the specific capacitance of the curve calculator was selected from all the constant current charge and discharge curves which are corresponding to 0.5 A/g, it was found that the Ni/C metal particles were 321.5 F/g. The specific capacitances of Cu/C, Co/C, Fe/C particles were measured corresponding to 46.7 F/g, 21.7 F/g and 168.8 F/g, respectively.

Fig. 8 reflects the specific capacitance of Ni/C, Cu/C, Co/C and Fe/C metal particles at different current densities. It can be seen that the specific capacitance of the Ni/C metal particles is the largest, followed by the Fe/C metal particles, and the smallest is the Cu/C metal particles. All CCMPs have similar shapes because they all have a special core-shell carbon sphere coating structure, and their special porous structure greatly enhances their specific surface area, resulting in a large increase in capacitance. However, the specific capacitance of carbon-coated different metal particles produced under the same conditions is different because the radius of the metal particles coated in the carbon layer is different, which affects the pore size of the carbon layer and the specific surface area.

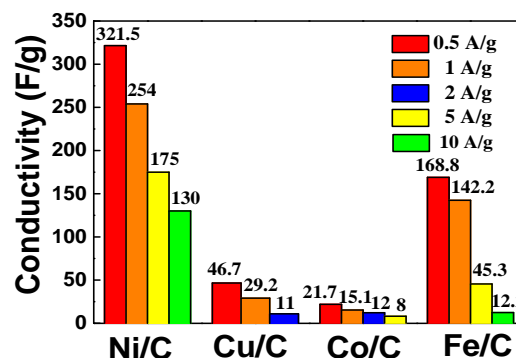


Fig. 8 Specific capacitance of Ni/C, Cu/C, Co/C and Fe/C metal particles at different current densities.

The A. C. Impedance test was also performed in the CHI760E electrochemical test system. Electrochemical Impedance Spectroscopy (EIS) has a test frequency of 0.01-10 Hz and a disturbance amplitude of 5 mV at open circuit voltage. Fig. 9 shows the electrochemical impedance spectra of Ni/C, Cu/C, Co/C and Fe/C. It is shown that the Nyquist characteristic curve of the product consists of a small semicircle and an inclined straight line. In the corresponding equivalent circuit diagram, R_s is solution resistance

and R_{ct} is charge transfer resistance. Table 1 shows the R_s and R_{ct} numerical charts of different carbon-coated metals (Ni, Cu, Co, Fe). In conclusion, this process is controlled by both electrochemistry and concentration polarization. The double-layer capacitive reactance arc appears in the high-frequency half-circle region, and displays a line along the imaginary axis in the low-frequency region. The diffusion control becomes stronger than the electrochemical control. Warburg impedance appears, which indicates its low electrolyte ion resistance and better capacitor behavior.

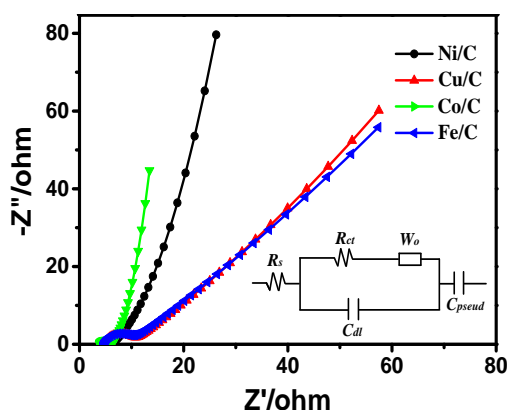


Fig. 9 Electrochemical impedance spectroscopy and equivalent circuit diagrams of carbon-coated metal particles.

Table 1 R_s and R_{ct} values of carbon-coated different transition metal (Ni, Cu, Co, Fe) particles.

Sample	Ni/C	Cu/C	Co/C	Fe/C
R_s (Ω)	4.499	3.389	5.104	4.801
R_{ct} (Ω)	1.577	2.092	4.959	4.741

IV. CONCLUSIONS

Carbon-coated transition metal (Ni, Co, Cu, Fe) particles were synthesized by hydrothermal method. The morphology and composition test results showed that the core-shell structure of the nanoparticles was carbon-coated, and the thin layer of the shell was amorphous carbon-coated. Cyclic voltammetry, constant current charge and discharge, and A.C. impedance in electrochemical operating systems have demonstrated that the particle materials have typical double-layer capacitance characteristics. It indicates that the Ni/C metal particles have higher specific surface area ($S_M = 241.80 \text{ m}^2/\text{g}$). Furthermore, the Ni/C particles exhibit superior capacitance characteristics, higher rate performance and low electrolyte ionic

resistance characteristics. The research of this kind of materials is of great significance not only for exploring high capacitance and capacitor materials, but also has broad application prospects in the field of photocatalysis.

ACKNOWLEDGMENTS

This research was supported by the Scientific Research Project of Hubei Provincial Department of Education (D20151506); Graduate Innovation Fund of Wuhan Institute of Technology (CX2017150).

REFERENCES

- [1]. FENG C, LIU X, SUN Y P, et al. Enhanced microwave absorption of flower-like FeNi@C nanocomposites by dual dielectric relaxation and multiple magnetic resonance. *Rsc Adv.*, 2014, 4(43):22710-22715.
- [2]. SHENG Q, SHEN Y, ZHANG J, et al. Ni doped Ag@C core-shell nanomaterials and their application in electrochemical H_2O_2 sensing. *Anal. Methods*, 2016, 9(1):1-7.
- [3]. CHEN F, XIE S, HUANG X, et al. Ionothermal synthesis of Fe_3O_4 magnetic nanoparticles as efficient heterogeneous Fenton-like catalysts for degradation of organic pollutants with H_2O_2 . *J. Hazard. Mater.*, 2016, 322(Pt A): 152-162.
- [4]. HE D C, FU Q M, MA Z B, et al. Facile synthesis and photocatalytic activity of ZnO/zinc titanate core-shell nanorod arrays. *Mater. Res. Express*, 2018, 5(2):025006-1-9.
- [5]. QIN Y H, XIONG Z Y, MA J, et al. Enhanced electrocatalytic activity and stability of Pd nanoparticles supported on TiO_2 -modified nitrogen-doped carbon for ethanol oxidation in alkaline media. *Int. J. Hydrogen Energy*, 2016, 42(2):1103-1112.
- [6]. SUN X. C, Gutierrez A, Yacamán M J, et al. Investigations on magnetic properties and structure for carbon encapsulated nanoparticles of Fe, Co, Ni. *Mater. Sci. Eng. A*, 2000, 286:157-160.
- [7]. ZUO Y, WANG G, PENG J, et al. Hybridization of graphene nanosheets and carbon-coated hollow Fe_3O_4 nanoparticles as a high-performance anode material for lithium-ion batteries. *J. Mater. Chem. A*, 2016, 4(7):2453-2460.
- [8]. ZHONG Z Y, CHEN H Y, TANG S B, et al. Catalytic growth of carbon nanoballs with and without cobalt encapsulation. *Chem. Phys. Lett.*, 2000, 330:41-47.
- [9]. TSAI S H, LEE C L, CHAO C W, et al. A novel technique for the formation of carbon-encapsulated metal nanoparticles on silicon. *Carbon*, 2000, 38(5):781-785.
- [10]. ELLO A, Fashedemi O O, Lektima J N, et al. High-performance symmetric electrochemical capacitor based on graphene foam and nanostructured manganese oxide. *Aip Adv.*, 2013, 3(8):1094-1103.
- [11]. LIANG J, CHEN S, XIE M, et al. Expedient fabrication of flower-like hierarchical

- mesoporous carbon superstructures as supercapacitor electrode materials. *J. Mater. Chem. A*, 2014, 2(40):16884-16891.
- [12]. JIAO J, Seraphin S, WANG X, et al. Preparation and properties of ferromagnetic carbon-coated Fe, Co, and Ni nanoparticles. *J. Appl. Phys.*, 1996, 80(1):103-108.
- [13]. ZHANG W M, WU X L, HU J S, et al. Carbon Coated Fe₃O₄ Nanospindles as a Superior Anode Material for Lithium-Ion Batteries. *Adv. Funct. Mater.*, 2010, 18(24):3941-3946.
- [14]. XIONG W, ZHOU L, LIU S. Development of gold-doped carbon foams as a sensitive electrochemical sensor for simultaneous determination of Pb (II) and Cu (II). *Chem. Eng. J.*, 2016, 284:650-656.
- [15]. FU G, CUI Z, CHEN Y, et al. Ni₃Fe-N Doped Carbon Sheets as a Bifunctional Electrocatalyst for Air Cathodes. *Adv. Energy Mater.*, 2017, 7(1):1601172-1-8.
- [16]. LONG Q, CHEN W, XU H, et al. Synthesis of functionalized 3D hierarchical porous carbon for high-performance supercapacitors. *Energy Environ. Sci.*, 2013, 6(8):2497-2504.
- [17]. Adhikari M P, Adhikari R, Shrestha R G, et al. Nanoporous Activated Carbons Derived from Agro-Waste Corncob for Enhanced Electrochemical and Sensing Performance. *J. Mater. Chem. A*, 2015, 88(8):1108-1115.
- [18]. WEN Z, ZHANG Y, WANG Y, et al. Redox transformation of arsenic by magnetic thin-film MnO₂, nanosheet-coated flowerlike Fe₃O₄, nanocomposites. *Chem. Eng. J.* 2017, 312:39-49.
- [19]. Inagaki M, Konno H, Tanaike O. Carbon Materials for Electrochemical Capacitors. *J. Power Sources*, 2010, 195(24):7880-7903.
- [20]. ZHAO Y, LIU M, GAN L, et al. Ultramicroporous Carbon Nanoparticles for the High-Performance Electrical Double-Layer Capacitor Electrode. *Energy Fuels*, 2014, 28(2):1561-1568.

Zixuan Fang "Preparation of carbon-coated metal particles and their electrochemical performance" *International Journal of Engineering Research and Applications (IJERA)*, Vol. 09, No.05, 2019, pp. 01-07